Nonlinear optical spectroscopy of excited states in polyfluorene

M. Tong, C.-X. Sheng, and Z. V. Vardeny*
Department of Physics, University of Utah, Salt Lake City, Utah 84112, USA
(Received 10 October 2006; revised manuscript received 16 January 2007; published 26 March 2007)

We used a variety of nonlinear optical (NLO) spectroscopies to study the singlet excited-state order and primary photoexcitations in polyfluorene, an important blue-emitting π-conjugated polymer. The polarized NLO spectroscopies include ultrafast pump-probe photomodulation in a broad spectral range of 0.2–2.6 eV, two-photon absorption in the range of 3.2–4.2 eV, and electroabsorption covering the spectral range of 2.8–5.0 eV. For completeness, we also measured the linear absorption and photoluminescence spectra. We found that the primary photoexcitations in polyfluorene are singlet excitons with ~100 ps lifetime that have a characteristic photomodulation spectrum comprising of two photoinduced absorption (PA) bands, PA_1 at 0.55 eV and PA_2 at 1.65 eV, and a strong stimulated emission band that peaked at ~2.5 eV. The two-photon absorption and electroabsorption spectra identify the exciton PA bands with optical transitions between the lowest-lying odd symmetry $1B_u$ exciton at 3.1 eV and two strongly coupled even symmetry states, namely, mA_g at 3.7 eV and kA_g at 4.7 eV. The excited state manifold also contains a strongly coupled odd symmetry exciton nB_u at 4.1 eV, which identifies the continuum band threshold. A polarization memory of ~2.1, typical to films of π-conjugated polymers, characterizes all three NLO spectra, reflecting the highly anisotropic third-order NLO coefficient, $\chi^{(3)}$ of the polymer chains. The four essential states, namely, $1A_g$, $1B_u$, mA_g, and nB_u, were used to satisfactorily fit the $\chi^{(3)}$ optical spectra using the summation over states model. The combination of the three NLO spectra and the model fit conclusively show that the band model, typical in inorganic semiconductors, cannot properly describe the poly(9,9-dioctylfluorene) polymer. On the contrary, a strongly bound exciton with intrachain binding energy of ~1 eV dominates the linear and NLO spectra of this polymer.

DOI: 10.1103/PhysRevB.75.125207 PACS number(s): 78.40.Me, 78.40.Fy, 78.47.+p

I. INTRODUCTION

π-conjugated polymers have emerged as a promising class of organic semiconductors due to their low processing cost and the broad range over which their optical and electronic properties may be chemically tuned.[1] Several device applications have been commercialized such as bright organic light-emitting diodes (OLEDs), with a variety of colors ranging from red to blue, and organic field-effect transistors; other applications have been investigated for commercialization such as white OLED, large-area photodetectors, organic photovoltaic cells, and current-injected lasers.[2,3] However, in spite of tremendous research of more than two decades, the photophysics of π-conjugated polymers is still hotly debated.[4] For example, it is still unclear whether the absorption spectrum of these materials is due to interband transition (namely, valence to conduction band), where photon absorption results in free carriers as in inorganic semiconductors,[5,6] or whether it is excitonic in nature as in molecular solids, resulting in singlet excitons as the primary photoexcitations.[7] It is generally accepted that photoluminescence (PL) in π-conjugated polymers is due to intrachain excitons rather than interband transition of photogenerated electrons (e) and holes (h). However, in films the formation of secondary interchain species that are nonradiative charge transfer excitons cannot be ruled out.[8] One of the reasons for this confusion is that many π-conjugated polymers show a branching ratio of photogenerated excitons and charge polarons following photon absorption.[9,10] This branching ratio has been invoked to be due to interchain interaction between adjacent chains,[11] which should decrease with larger interchain separation when bulky side groups are involved in the polymer structure.

Polyfluorene is an attractive material for display applications due to efficient *blue emission*[12] and relatively large hole mobility with trap-free transport.[13] Poly(9,9-dioctylfluorene) (PFO) (shown in Fig. 1 inset) exhibits a complex morphological behavior that has had interesting implications for its photophysical properties.[14,15] It was previously shown that the structural versatility of PFO can be exploited in manipulating the sample's electronic and optical properties.[14,16] When changing a pristine sample with a glassy structure, dubbed α phase, into a film with more superior order, dubbed β phase, the hole mobility increases,[16] laser action occurs at reduced excitation intensities, and spectral narrowing is obtained at several wavelengths.[17] However, even in the disor-

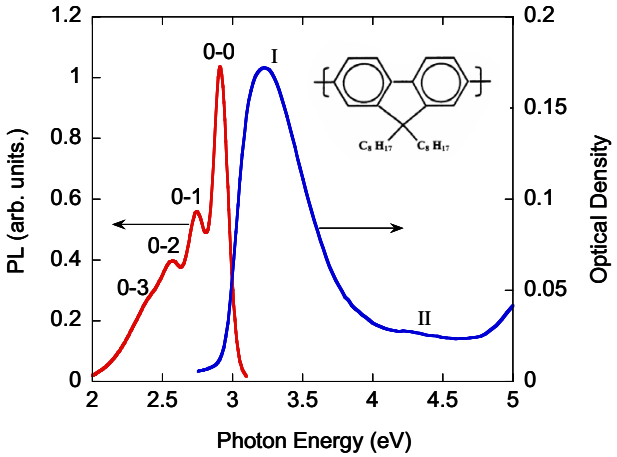

FIG. 1. (Color online) The normalized absorption and photoluminescence emission spectra of a PFO film in the glassy α phase. The polymer repeated unit is shown in the inset.

dered α phase, PFO shows a relatively high degree of planarity, which together with the bulky side group should provide a clean case for studying intrachain photoexcitations and characteristic excited states with only a small contribution due to interchain interaction. Nevertheless, several early studies of ultrafast photoexcitation dynamics in PFO led to confusing results. In one study of oriented PFO,[18] three types of photoexcitations were invoked: hot carriers, excitons, and charge polarons. In two other studies,[19,20] both excitons and bound polaron pairs were shown to simultaneously coexist. Under these circumstances, it is difficult to decide whether PFO excited states are "bandlike" or "excitonic" in nature. Some of the reasons for this confusion include the relatively narrow spectral range in which PFO photoexcitations were previously probed, the high excitation intensity used, as well as the lack of other complementary optical measurements to fully understand the excited-state nature of this polymer. In the quest of understanding the singlet manifold in PFO, more recent studies focused on three-beam excitation,[21–23] where the role of even parity states was emphasized. In these studies, it was realized that when excited deeper into the singlet manifold, charge species were then primarily photogenerated; however, most of them geminately recombined within a few picoseconds.

In the present work, we employ a variety of nonlinear optical (NLO) spectroscopies to elucidate the photoexcitations and important excited states in the singlet manifold of the PFO polymer. The NLO spectroscopies include ultrafast polarized pump-probe photomodulation (PM), electroabsorption (EA), and two-photon absorption (TPA); we complete the optical investigation by comparing the NLO spectra with linear optical measurements that include absorption and PL spectra. TPA spectroscopy is sensitive to excited states with even, or A_g, symmetry, and thus is complementary to linear absorption that probes excited states with odd, or B_u, symmetry. EA spectroscopy is sensitive to excited states of both B_u and A_g symmetries. The TPA spectrum was measured before in another PFO derivative in solution,[24] whereas the EA spectrum was measured in a PFO film that underwent several phase transitions;[14] also, the spectrum was analyzed in terms of first and second derivatives of the absorption spectrum, without underlying the role of specific electronic excited states in the polymer chain. The application of various NLO and linear spectroscopies to the *same* polymer film has provided us here with a more complete picture of the electronic states in PFO compared to that in previous works.

The NLO spectra were analyzed in terms of several essential excited states[25] that are strongly coupled to each other and to the ground state, namely, $1B_u$, mA_g, nB_u, and kA_g excitonic states, using the summation over states method;[26] a consistent and elegant picture for PFO electronic states has emerged. We found that the primary photoexcitations in PFO are singlet excitons with two photoinduced absorption (PA) bands in the mid- and near-IR spectral ranges and a strong stimulated emission (SE) band in the visible range. The PA bands can be understood[27] to result from optical transitions in the singlet manifold, namely, $1B_u \rightarrow mA_g$ and $1B_u \rightarrow kA_g$, and SE from the $1B_u$ to the ground (or $1A_g$) state. We conclude that the PFO excited state manifold is composed of several excitonic states with B_u and A_g symmetries, rather than a continuum band that characterizes regular semiconductors. From our experimental results, we infer that the lowest intrachain excited electronic state in PFO is a strongly bound exciton ($1B_u$) having an intrachain binding energy of $\sim$1 eV.

II. EXPERIMENT

The transient PM spectrum in PFO films was studied using the polarized pump-probe correlation technique with $\sim$150 fs time resolution. For the present studies, we utilized two femtosecond Ti:sapphire laser systems with low and high repetition rates, having high and low pulse energies, respectively.[7] These two laser systems separately cover the mid- and near-IR spectral ranges; the high repetition laser system was used in the mid-IR range,[20] whereas the low repetition laser system was used in the near-IR and visible spectral range.[28] The pump pulses were kept fixed at 3.1 eV for both laser systems. The PM spectra obtained using the two laser systems were then normalized to each other in the visible range (2 eV), thus providing a very broad probe spectral range from 0.15 to 2.6 eV with small spectral gaps.

The low repetition rate high-energy laser system was a homemade Ti:sapphire regenerative amplifier that provides pulses of 120 fs duration at photon energies of 1.55 eV, with 400 μJ energy per pulse at a repetition rate of 1 kHz. The second harmonic of the fundamental pulses at 3.1 eV was used as the pump beam. The probe beam was a white light "supercontinuum" with a spectral range of 1.2–2.7 eV, which was generated using a portion of the Ti:sapphire amplifier output in a 1-mm-thick sapphire plate. An overall time resolution of $\sim$150 fs in the pump-probe measurements was achieved by adjusting the stage to compensate the spectral chirp as measured by time-resolved TPA (see below). The probe beam polarization was set to be either parallel or perpendicular to the pump beam polarization. For improving the signal-to-noise ratio, the pump beam was synchronously modulated by a mechanical chopper at exactly half the repetition rate of the Ti:sapphire laser system ($\sim$500 Hz). The probe beam was mechanically delayed with respect to the pump beam using a computerized translation stage in the time interval t up to 200 ps. The delay line that corresponds to $t=0$ was set by a sum frequency cross-correlation trace of the pump and probe pulses in a NLO crystal.

Since some of the photoexcitation dynamics depend on the excitation density, care was taken in the experimental design to minimize distortion of the measured pump-probe response by spatial inhomogeneity of the photoexcitation distribution. Therefore, the pump beam was focused onto the sample to a 1 mm diameter round spot, whereas the probe beam was focused using an achromatic lens onto a 0.4 mm diameter spot in the center of the pump illuminated spot. To ensure the reproducibility of the alignment, the spatial overlap of the pump-probe beams was set using a telescopic microscope. The wavelength resolution of this system was about 4 nm using a 1/8 m monochromator with a 0.6 mm exit slit, which was placed in the probe beam after it passed through the sample. The transient spectrum of the photoinduced change (ΔT) in the sample transmission (T) was ob-

tained using a phase-sensitive technique. Following pump photon absorption, the probe beam experiences PA, which is represented in the spectra as negative differential transmittance $-\Delta T/T$. Since the pump and probe beams are linearly polarized, we could measure ΔT_{pa} (ΔT_{pe}), where the pump and probe polarizations are parallel (perpendicular) to each other.[28] Pump-induced SE and photobleaching (PB) of the optical absorption in the ground state with $\Delta T>0$ were also obtained.[27] In the small signal limit, $\Delta T(t)$ is expected to be proportional to the photoexcitation density $N(t)$, which for an optically thick film is given by the relation $\Delta T/T=N\sigma/\alpha_L$, where σ is the photoexcitation optical cross section and α_L is the absorption coefficient at the pump laser excitation wavelength. To correct the pump-probe signal for intensity fluctuations in the supercontinuum at the selected probe wavelength, the probe signal was normalized by a reference signal at each delay time [this technique was dubbed as "A-B" (Ref. 29)] with a significant improvement in the measured signal-to-noise ratio, giving a sensitivity of $\Delta T/T=10^{-4}$ that corresponds to a photoexcitation density of $\sim 10^{17}$ cm^{-3}.

The high repetition rate low-energy laser system was an optical parametric oscillator (OPAL, Spectra Physics) that was pumped by a 100 fs Ti:sapphire laser oscillator (Tsunami, Spectra Physics) at a repetition rate of about 80 MHz.[28] The pump beam was extracted from the laser oscillator and was frequency doubled to 3.1 eV. The probe beam was extracted from the signal and idler beams of the optical parametric oscillator in the spectral ranges of 0.56–0.68 and 0.94–1.02 eV, respectively, with about 150 fs time resolution. We extended the spectral range deeper into the IR using a difference frequency setup in a NLO crystal. When using the signal and idler beams and changing the central frequency of the optical parametric oscillator (OPO) to 1.55 μm, we could then extend the spectral range between 0.15 and 1.05 eV, with a few remaining gaps in the spectrum.[7] This laser system provides low-intensity measurements, where the pump intensity ranges from 0.1 to 30 μJ/cm^2 per pulse, with $\Delta T/T$ resolution of $\sim 10^{-6}$ that corresponds to photoexcitation density of $\sim 10^{15}$ cm^{-3}.

PFO powder was purchased from ADS (in Canada) and was used to make films either by drop cast or by spin cast on sapphire substrates, without further purification. For the pump-probe studies, all measurements were carried out at room temperature in a cryostat that provided a dynamical vacuum of 100 μTorr to prevent polymer film degradation due to the strong laser illumination at ambient conditions.[30] Pump-probe signals were measured over a range of pump intensities to ensure linearity of the $\Delta T/T$ response with respect to the initial photoexcitation density; we thus worked at intensities below 300 μJ/cm^2 per pulse, with typical intensities of about 30 μJ/cm^2 to prevent signal saturation.

The TPA spectrum was measured using the polarized pump-probe correlation technique with the low repetition rate high-energy laser system at time delay $t=0$. The linearly polarized pump beam was set at 1.55 eV, below the polymer absorption band, whereas the probe beam from the white light supercontinuum covered the spectral range from 1.6 to 2.6 eV. The temporal and spatial overlaps between the pump and probe beams on the sample film lead to a PA signal that peaks at $t=0$. We interpret it here as due to TPA of one pump photon with one probe photon.

For the EA measurements, we used a PFO film spin cast on a substrate with patterned metallic electrodes.[26] The EA substrate consisted of two interdigitated sets of a few hundred gold electrodes 30 μm wide patterned on a sapphire disk $\sim$1 mm thick. The sample was placed in a cryostat for low-temperature measurements. An electric field was generated in the sample by applying a potential V to the electrodes. An applied potential $V=300$ V (typical in our experiments) resulted in field strength $F=1\times 10^5$ V/cm. We varied V on the electrodes using a sinusoidal signal generator at $f=1$ kHz and a simple transformer to achieve high voltages. For probing of the EA spectrum, we used an incandescent light source from a Xe lamp, with broadband visible and ultraviolet spectra ranging from 2.6 to $\sim$5.0 eV. The light beam was dispersed through a monochromator, focused on the sample, and detected by a UV-enhanced silicon photodiode. The modulation ΔT of the transmission T is expected to be the same for positive and negative V since the polymer chains are not preferentially aligned with respect to the electrodes. Thus, we measured ΔT using a lock-in amplifier set to twice the frequency ($2f$) of the applied field.[26] We verified that no EA signal was observed at f or $3f$. ΔT and T spectra were measured separately using a homemade spectrometer that consisted of a $\frac{1}{4}$ m monochromator equipped with several gratings and solid-state detectors for spanning the EA in the broadest spectral range. The EA spectrum was obtained from the ratio $\Delta T/T$, which was measured at various applied voltages and polarizations of the probe light with respect to the direction of the applied field.

III. RESULTS AND DISCUSSION

A. Absorption and PL spectra

The PFO polymer repeat unit is shown in the inset of Fig. 1. The polymer chain is highly planar even in the disordered α phase since the two repeated benzene rings are tied together with two large adjacent side groups. The room-temperature absorption and PL spectra are shown together in Fig. 1 for ease of comparison. The main absorption band peaks at 3.2 eV with an onset at $\sim$2.95 eV; however, it is featureless and thus gives the impression of a smooth absorption spectrum, similar to that typical of inorganic semiconductors. The PL spectrum has a relatively small redshift with respect to the absorption band, but exhibits a clear vibronic structure with peaks at about 2.90 (0-0), 2.72 (0-1), and 2.55 (0–2) eV; a fourth phonon side band (0-3) may be seen at $\sim$2.37 eV. The vibrational series in the PL spectrum shows that the polymer possesses strong electron-phonon coupling to a strongly coupled vibration (identified as the C=C stretching at $\sim$185 meV), which, however, is not clearly seen in the absorption spectrum. The reason for the apparent dissimilarity between the PL and absorption spectra is the existence of a broad distribution of the polymer conjugation length (CL) in the sample film, where the characteristic optical energy gap of the chains depends inversely on the CL. Whereas the absorption process occurs in all chains, the cw PL is preferentially emitted from the longest chains in the film having the smallest optical gap that collects most of the diffusing excitons, and thus the phonon side bands seen in

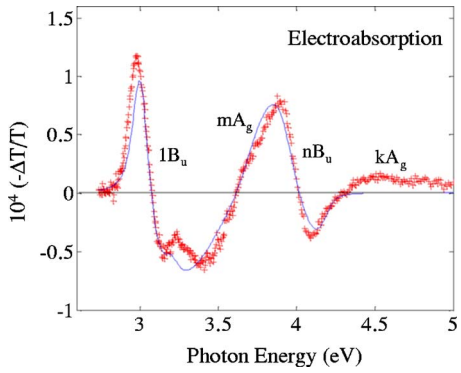

FIG. 2. (Color online) PFO electroabsorption spectrum (red, crosses) and the fit (blue, full line) using the SOS model with fitting parameters given in Table I. The essential states $1B_u$, mA_g, nB_u, and kA_g are assigned.

the PL spectrum are mainly related to these long chains. We therefore conclude that the smooth absorption spectrum has little to do with interband transition but, in fact, is an inhomogeneous broadened version of delocalized π-π^* transitions involving optical transitions from the ground state ($1A_g$) to the first odd-parity exciton ($1B_u$).[31] It is interesting to note that the absorption spectrum also contains a small feature at ~4.1 eV; this feature is enhanced, and thus seen more clearly in the EA spectrum (see below).

B. Electroabsorption spectroscopy

To elucidate the nature of the excited states responsible for the broad optical absorption band in the PFO film, we applied the EA spectroscopy. EA has provided a sensitive tool for studying the band structure of inorganic semiconductors,[32] as well as their organic counterparts.[33–35] Transitions at singularities of the joint density of states respond particularly sensitively to an external field and are therefore lifted from the broad background of the absorption continuum. The EA sensitivity decreases, however, in more confined electronic materials, where electric fields of the order of 100 kV/cm are too small of a perturbation to cause sizable changes in the optical spectra. As states become more extended by intermolecular coupling, they respond more sensitively to an intermediately strong electric field F since the potential variation across such states cannot be ignored compared to the separation of energy levels. EA may selectively probe extended states and is thus particularly effective for organic semiconductors, which are traditionally dominated by excitonic absorption. One of the most notable examples of the application of EA spectroscopy to organic semiconductors is polydiacetylene, in which EA spectroscopy was able to separate absorption bands of quasi one-dimensional (1D) excitons from that of the continuum band.[36] The confined excitons were shown to exhibit a quadratic Stark effect, where the EA signal scales with F^2 and the EA spectrum is proportional to the derivative of the absorption with respect to the photon energy $[\partial\alpha/\partial\omega(\omega)]$. In contrast, the EA related to the continuum band scales with $F^{1/3}$ and shows Franz-Keldysh (FK)-type oscillation in photon energy. The separation of the EA contribution of excitons and the continuum band was then used to obtain the exciton binding energy in polydiacetylene, which was found to be ~0.5 eV.[36]

Figure 2 shows the EA spectrum of a PFO film on a sapphire substrate up to 5.0 eV at field value F of 10^5 V/cm. The EA spectrum was measured at 80 K to decrease the thermal effect contribution, which also scales with F^2 similar to that of the EA itself [see Fig. 3(a) inset]. There are several spectral features in the EA spectrum: a first-derivative like feature with zero crossing at ~3.1 (assigned as $1B_u$), a modulation feature that does not resemble a derivativelike feature with zero crossing at 4.0 and 4.3 eV (assigned as nB_u), two well-resolved phonon side bands related to the $1B_u$ at 3.2 and 3.45 eV, and two induced absorption bands at 3.7 eV (assigned as mA_g) and 4.5 eV (assigned as kA_g). No FK-type oscillation related to the onset of the interband transition is seen in the EA spectrum here. The most prominent characteristic properties of a FK oscillation feature is its spectral broadening with the electric-field strength F and the dependence on $F^{1/3}$.[36] Figure 3(a) shows that the EA spectrum does not change much with F, and the entire spectrum

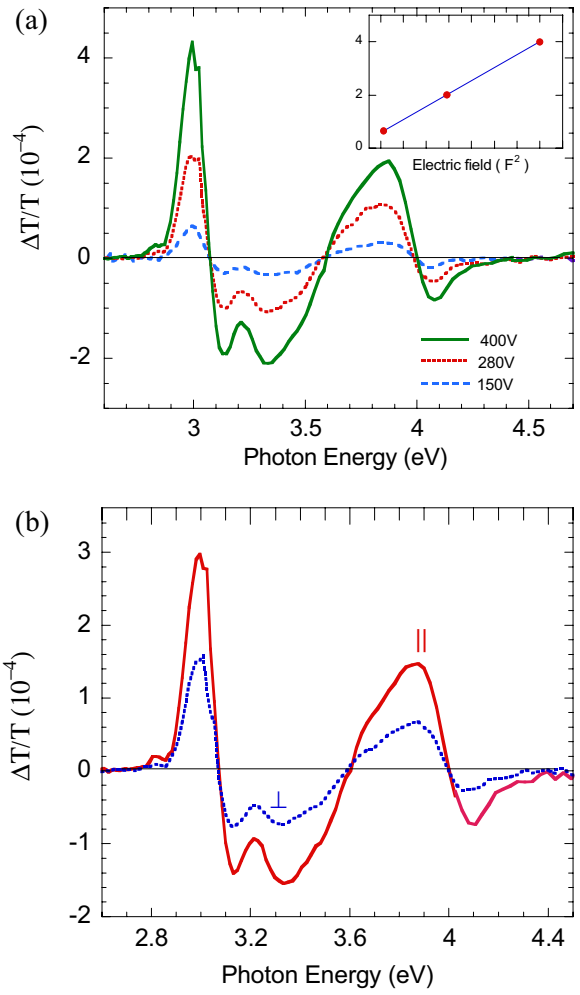

FIG. 3. (Color online) (a) PFO EA spectrum at three different applied voltages V resulting in three different field strengths F. The inset shows the dependence of the EA signal on V^2. (b) PFO polarized EA spectrum with light polarization parallel (red, full line) and perpendicular (blue, dashed line) to the applied electric field vector.

also scales with F^2 [Fig. 3(a) inset], in contrast to the expectation of the FK EA feature. We thus conclude that PFO excited states are better described in terms of excitons, rather than in the language of band-to-band transition typical of inorganic semiconductors. We also measured the polarization dependence of the EA spectrum [Fig. 3(b)]. We found that the EA spectrum parallel to the direction of the applied field is ~2.1, larger than that perpendicular to the field, but otherwise, the two spectra are very similar to each other.

We interpret the EA spectrum as follows.[26,35] The first-derivative-like feature at ~3.1 eV is due to a Stark shift of the lowest-lying exciton, namely, the $1B_u$. The modulation feature centered at ~4.1 is due to the electric-field-induced shift of the most strongly coupled exciton to the mA_g, namely, the nB_u, which is very close to the continuum band onset.[35] The derivative-, wigglylike feature at energies just above $E(1B_u)$ is due to the Stark shift of the $1B_u$-related phonon side bands. These features are more easily observed in EA than in the linear absorption spectrum because of the strong dependence of the exciton polarizability on the CL in the polymer chains. The polarizability was shown[37] to increase as $(\mathrm{CL})^n$, where $n \sim 6$, and thus the EA spectrum preferentially focuses on long CL, similar to the case of the PL spectrum discussed above. The EA-induced absorption feature at 3.7 eV does not have any corresponding spectral feature in the linear absorption spectrum. We therefore conclude that this feature in the EA spectrum involves a strongly coupled A_g state, dubbed mA_g.[35] Such a state would not normally show up in the linear absorption spectrum since the optical transition $1A_g \rightarrow mA_g$ is strictly forbidden. The presence of this band in the EA spectrum can be explained by the electric field effect on the film, which breaks the symmetry, resulting in the transfer of oscillator strength from the allowed $1A_g \rightarrow 1B_u$ transition to the forbidden $1A_g \rightarrow mA_g$ transition.[25] The same applies for the EA feature at ~4.5 eV assigned as kA_g.[27] This is another strongly coupled A_g state that is further away from the $1B_u$; however, it may belong to a different exciton manifold altogether.[38,39]

Electroabsorption is a third-order NLO effect and thus can be described by the third-order optical susceptibility, namely, $\chi^{(3)}(-\omega;\omega,0,0)$ (Refs. 25 and 35):

$$-\Delta T/T = \frac{4\pi\omega}{nc}\,\mathrm{Im}[\chi^{(3)}(-\omega;\omega,0,0)]F^2 d, \qquad (1)$$

where d is the film thickness, n is the refractive index, c is the speed of light, and ω is the optical frequency; the field modulation $f \ll \omega$, and this explains the zero frequency for $\chi^{(3)}$ in Eq. (1). The relation between the EA and $\chi^{(3)}$ in Eq. (1) shows that the polarization dependence of the EA spectrum is, in fact, related to the anisotropy of $\chi^{(3)}$ of the PFO chains in the film. The obtained polarization of ~2:1 is thus not surprising since the PFO polymer chains are quite anisotropic, with NLO coefficient that is stronger along the polymer chains. In fact, the theoretical limit for a $\chi^{(3)}$ process in polymers, where the excited and ground states have parallel vector dipole moments, is 3.[28] So PFO is not far from that limit. We thus expect similar anisotropy to hold for the other NLO measurements described here, which can be also described by a $\chi^{(3)}$ process.

In order to obtain more quantitative information about the main exciton states in PFO chains, we fitted the EA spectrum using a model calculation. For this fit, we calculated the $\chi^{(3)}$ spectrum [Eq. (1)] using the summation over states (SOS) model originally proposed by Orr and Ward,[40] further developed for π-conjugated polymers by Mazumdar and co-workers,[25,35] and implemented in a variety of conducting polymers by Liess *et al.*[26] In this model the $\chi^{(3)}$ spectrum is a summation of 16 terms, each containing a denominator that is proportional to the multiplication of several dipole moment transitions μ_{ij}, such as from the ground states $1A_g$ to $1B_u$ ($1A_g \rightarrow 1B_u$, with strength μ_{01}) and $1B_u$ to mA_g ($1B_u \rightarrow mA_g$, with strength μ_{12}), and a nominator that is resonant at energies related to the main essential states [see Eqs. (3)–(12) in Ref. 26]. Apart from the kA_g state[38] and according to the "essential state picture" in π-conjugated polymers advanced by Mazumdar and co-workers,[25,35] there are *four* essential states that contribute substantially to the main EA spectral features in these compounds; these are $1A_g$, $1B_u$, mA_g, and nB_u. This is justified in π-conjugated polymers since these four states are most strongly coupled to each other; the other B_u and A_g exciton states in the singlet manifold have very small transition dipole moments.[35]

Out of the SOS terms, there are four main classes of terms [(a)–(d)] that indicate the channel taken by the dipole moment transitions. One such class is (a) the channel ($1A_g \rightarrow 1B_u \rightarrow 1A_g \rightarrow 1B_u \rightarrow 1A_g$) that involves only the $1A_g$ and $1B_u$ states. This channel gives a Stark shift of the opposite sign for the $1B_u$ exciton in the spectrum (i.e., blueshift) in contrast to the redshift observed in the experiment. The other term of the same type (b) involves the transition $1A_g$ to nB_u ($1A_g \rightarrow nB_u$), which is too small in the SOS calculation. Channel (c) involves both $1B_u$ and mA_g ($1A_g \rightarrow 1B_u \rightarrow mA_g \rightarrow 1B_u \rightarrow 1A_g$). This channel gives the correct sign to the $1B_u$ Stark shift (that is redshift) and is usually larger than terms (a) and (b) in the SOS since $\mu_{12} > \mu_{01}$. The last channel (d) involves *all four* essential states via the process $1A_g \rightarrow 1B_u \rightarrow mA_g \rightarrow nB_u \rightarrow 1A_g$. This term gives the correct sign (that is redshift) to the nB_u state in the EA spectrum if one of the dipole moment transitions involved (μ_{23} for $mA_g \rightarrow nB_u$ or μ_{03} for $nB_u \rightarrow 1A_g$) is negative. In reality,[35] the nB_u redshift is explained to be due to its strong coupling to the continuum band lying above it in energy, which contains both alternate A_g and B_u states that are very close to each other; thus, term (d) with a negative transition dipole moment mimics this strong coupling in the SOS model.[35]

The kA_g exciton does not belong to the same exciton manifold as that of the other four essential states.[39] In fact, kA_g is composed of π-π^* states that are combinations of localized and delocalized states, whereas the four essential states belong to delocalized π-π^* states alone.[38,39] We therefore have not taken the kA_g into account in our model calculation, and thus the model used here cannot reproduce its EA feature (see Fig. 2).

The essential state energies and their dipole moment transitions were taken as free parameters in the SOS fit (see Table I). In the fitting, we also took into account the main phonon side bands, with phonon frequency of ~185 meV for

TABLE I. The best fitting parameters for the EA spectrum of PFO using the SOS model with four essential states, namely $1A_g$ (assigned the number 0), $1B_u$ (assigned 1), mA_g (assigned 2), and nB_u (assigned 3), as well as a CL distribution and most strongly coupled phonon. The parameters are described in detail in Ref. 24 and include the essential state energies with respect to $E(1A_g)$, as well as their relative displacements Δq and transition dipole moments μ_{ij}. The $h\nu$ phonon is the frequency of the most strongly coupled vibration, and the CL distribution is characterized by the width γ and asymmetry η.

$E(1B_u)$ (eV)	3.1
$\Delta q_1 = q(1B_u) - q(1A_g)$	0.7
$E(mA_g)$ (eV)	3.7
$\Delta q_2 = q(mA_g) - q(1B_u)$	−0.5
$E(nB_u)$ (eV)	4.1
$\Delta q_3 = q(nB_u) - q(mA_g)$	0.6
$h\nu$ phonon (eV)	0.185
CL distribution width γ (eV)	0.2
CL distribution asymmetry η	5.0
Transition dipole moment:	
μ_{01} $(1A_g \rightarrow 1B_u)$	1.0
μ_{12} $(1B_u \rightarrow mA_g)$	2.1
$\mu_{23}\mu_{30}$ $(mA_g \rightarrow nB_u \rightarrow 1A_g)$	−1.8

the most strongly coupled intrachain vibration (the C=C stretching mode), as well as an asymmetric CL distribution function.[26] The phonon side bands and the CL distribution were shown to be very important in fitting the EA spectra of many π-conjugated polymers.[26] The solid line in Fig. 2 shows the best fit to the EA spectrum, as obtained using the SOS with parameters given in Table I. The agreement between the model calculation and experimental spectra is very good. From Table I, we get the energies of the most strongly coupled excitons in PFO as follows: $E(1B_u)=3.1$ eV, $E(mA_g)=3.7$ eV, and $E(nB_u)=4.1$ eV. Furthermore, from the EA spectrum at energies above $E(nB_u)$, we approximate $E(kA_g)=4.7$ eV.[38] These major states play a dominant role in the other two NLO spectroscopies, namely, the TPA and transient PM spectra, as discussed below. From Table I, we also get the transition dipole moment between the essential states. Indeed, we see from the fitting that the transition dipole moments $\mu_{12} > \mu_{01}$, which explains the $1B_u$ Stark shift to lower energies, whereas $\mu_{23}\mu_{03} < 0$, which explains the nB_u negative Stark shift in the EA spectrum.

From the magnitude of the EA signal compared to the first derivative of the absorption spectrum, an estimate of the difference in polarizability Δp between the ground and the first excited states, namely, the $1B_u$ may be obtained.[14,26] This requires a careful fit to the absorption spectrum using the same parameters that were used to fit the EA spectrum and a different CL distribution function.[26] Instead, we estimate Δp from a simple comparison of the PFO EA spectrum to that of various polymers for which Δp is known.[26] We obtained a polarizability difference between $1A_g$ and $1B_u$ states, $\Delta p \sim 5000$ Å^3, in fair agreement with a previous estimate.[14]

It is known that the continuum band in π-conjugated polymers is very close to $E(nB_u)$ (Ref. 35); it is thus tempting to identify the transition from the ground state into the continuum band in the linear absorption spectrum. Based on the EA spectrum at ~4.1 eV and its analysis in terms of $E(nB_u)$, we then tentatively assign absorption band II in the linear absorption spectrum (Fig. 1) at ~4.1 eV as the optical transition $1A_g \rightarrow nB_u$ (or continuum band onset). We estimate the absorption strength ratio of bands I and II in the linear absorption spectrum (Fig. 1) to be ~100:1. It is well established that in semiconductors, the interband transition strength substantially decreases relative to the exciton transition strength for large exciton binding energy E_b.[35,36] The large ratio obtained between bands I and II in the absorption spectrum thus indicates that E_b in PFO is relatively large, i.e., of the order of 1 eV. Actually, we may estimate E_b of the lowest-lying singlet exciton in PFO from the relation $E(nB_u) - E(1B_u)$. From the values given in Table I, we get a large binding energy $E_b \approx 1$ eV. This large E_b is not unique in the class of π-conjugated polymers. It is similar to E_b extracted for MEH-PPV ($E_b \approx 0.8$ eV) when using the corresponding EA spectrum.[26] The large value for E_b shows that electron-hole interaction and electron correlation[15] are relatively large in PFO and do not permit us to describe this polymer in terms used by the semiconductor band model.[4]

C. Two-photon-absorption spectroscopy

In π-conjugated polymers the optical transitions between the ground state $1A_g$ and the B_u excitonic states are allowed; in particular, the transition $1A_g \rightarrow 1B_u$ dominates the absorption spectrum.[41,42] On the contrary, the optical transitions from $1A_g$ to any other state with A_g symmetry are strictly forbidden. However, these optical transitions are allowed in TPA.[25] Therefore, TPA spectroscopy has been used in the class of π-conjugated polymers to get information about the A_g energies in these materials.[43,44] This information is important since transitions of photogenerated $1B_u$ excitons to A_g states are dipole allowed and thus dominate the PA spectrum of $1B_u$ excitons in these polymers.[45] In addition, it was also found[46] that the resonant Raman scattering dispersion known to exist in π-conjugated polymers surprisingly depends on the lowest-lying A_g states, rather than on the B_u states, and thus $E(A_g)$ are worthy to determine in this class of materials.

Usually, the TPA spectrum has been measured in π-conjugated polymers either directly by techniques such as optical absorption at high excitation intensity,[47,48] and Z scan,[49,50] or indirectly by measuring the fluorescence emission following TPA at high intensity, a technique dubbed "two-photon-fluorescence."[51] Typically, two TPA bands are observed in π-conjugated polymers, namely, mA_g and kA_g, where $E(mA_g) < E(kA_g)$.[43] It is worth mentioning that in nonluminescent π-conjugated polymers, such as t-$(CH)_x$ (Ref. 47) and polydiacetylene,[48] it was measured that $E(2A_g) < E(1B_u)$. In this case the photogenerated $1B_u$ excitons quickly undergo internal conversion into the lowest-energy exciton, which is the $2A_g$; consequently, the transient PL emission is very fast, i.e., of the order of 200 fs. However, it has been found[43] that the $2A_g$ state is not easy to detect by NLO techniques since it is not strongly coupled to any B_u states, and thus is very weak in both TPA and EA spectra.

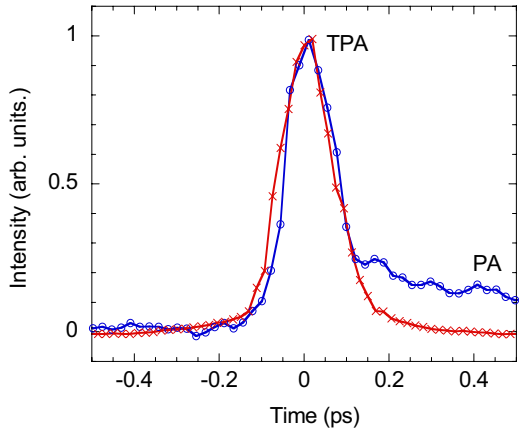

FIG. 4. (Color online) PFO transient TPA trace (blue line, circles) involving the pump (at 1.55 eV) and probe (at 1.9 eV) pulses, compared to the pump-probe cross correlation trace (red line, crosses) measured using a NLO crystal. The relatively long-lived PA plateau is due to the PA related photoexcitations generated by TPA from the pump pulses (see text).

In the present work, we have chosen to measure the TPA spectrum using the pump and probe techniques at time $t=0$. The linearly polarized pump beam from the low repetition high power laser system was set *fixed* at 1.55 eV, which is below the polymer main absorption band, whereas the probe beam from the white light supercontinuum with polarization either parallel or perpendicular to that of the pump beam spreads the pump-probe spectral range from 1.6 to 2.6 eV, thus covering the TPA photon energy from 3.15 to 4.15 eV. If only the linear absorption is considered, then the pump beam alone at 1.55 eV is unable to generate photoexcitations above the gap since its photon energy is much smaller than the optical gap of PFO at ~3.0 eV. However, the temporal and spatial overlaps between the pump and probe beams lead to a transient PA signal that peaks at $t=0$. As seen in Fig. 4, for a probe photon energy of ~1.9 eV, this PA has a temporal profile similar to the cross-correlation function of the pump and probe pulses, which we interpret here as due to TPA of one pump photon with one probe photon. The long temporal tail seen in Fig. 4 at times t longer than that of the cross-correlation function is caused by PA of photoexcitations that are generated due to the TPA of the pump pulses alone.[22] This tail was subtracted out from the transient response at $t=0$ for obtaining the TPA spectrum clearly from the PA due to the TPA-related photoexcitations. Otherwise, the TPA related to the pump pulses does not directly influence the transmission of the probe pulses. Two separate TPA spectra were obtained, where the probe beam polarization was set either parallel or perpendicular to the pump beam polarization.

Figure 5(a) shows the TPA spectrum of the PFO film up to 4.4 eV compared with the linear absorption spectrum. The TPA shows a relatively broad band [full width at half maximum (FWHM) of ~0.4 eV] peaked at 3.7 eV, which has a comparable width to that of the linear absorption band. We interpret the TPA band at 3.7 eV as the inhomogeneously broadened mA_g state in PFO,[24,45] in agreement with the EA spectra discussed above (see Table I). We emphasize that the

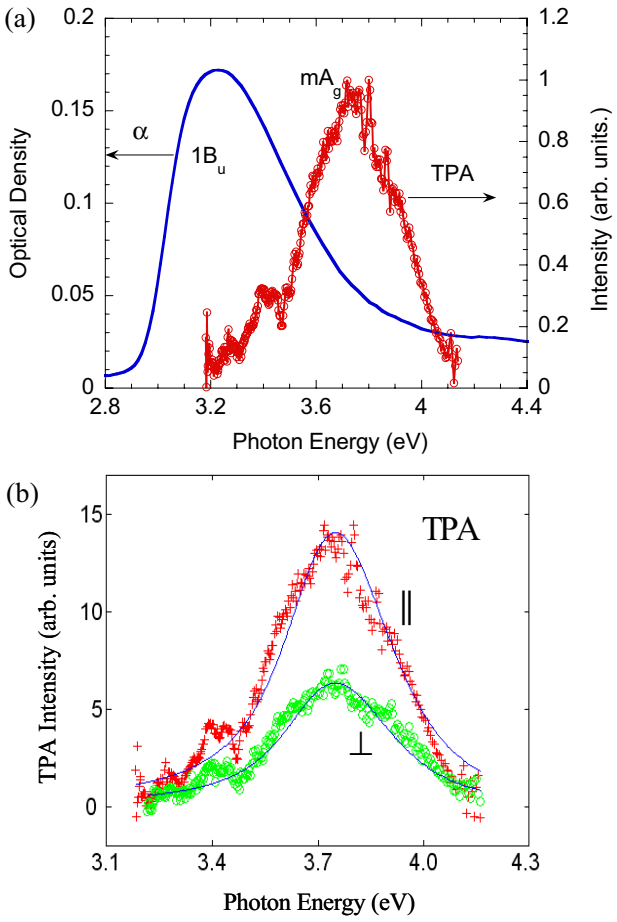

FIG. 5. (Color online) (a) The two-photon absorption (TPA) spectrum of PFO compared to the linear absorption spectrum. The essential states $1B_u$ and mA_g are assigned. (b) PFO TPA spectrum measured with pump and probe polarizations either parallel (red, crosses) or perpendicular (green, circles) to each other. The line through the data points is a fit using the SOS model with parameters given in Table I.

TPA spectrum has zero strength at 3.2 eV, which is at the photon energy where the linear absorption spectrum has a maximum. In the semiconductor band model, the valence band (VB) and conduction band (CB) are composed of states of both odd and even symmetries that form a continuum band. In this case, the TPA and linear absorption spectra overlap, or have very little difference, perhaps because of slightly different optical dipole moments.[38,43] In contrast, it is apparent that the TPA and linear absorption spectra *do not overlap* in PFO; in fact, there is ~0.5 eV energy difference between their respective maxima [Fig. 5(a)]. This is *compelling evidence* that the semiconductor band model *cannot* properly describe the PFO excited states. On the contrary, the energy difference between the linear and TPA spectra of ~0.5 eV sets the lower limit for the exciton binding energy in this polymer, in agreement with E_b extracted above from the EA spectrum.

Figure 5(b) shows the polarization anisotropy in the TPA spectrum. The parallel and perpendicular TPA spectra differ by a factor of ~2.2, but otherwise, they show the same spectral features. The polarization anisotropy found in TPA is in

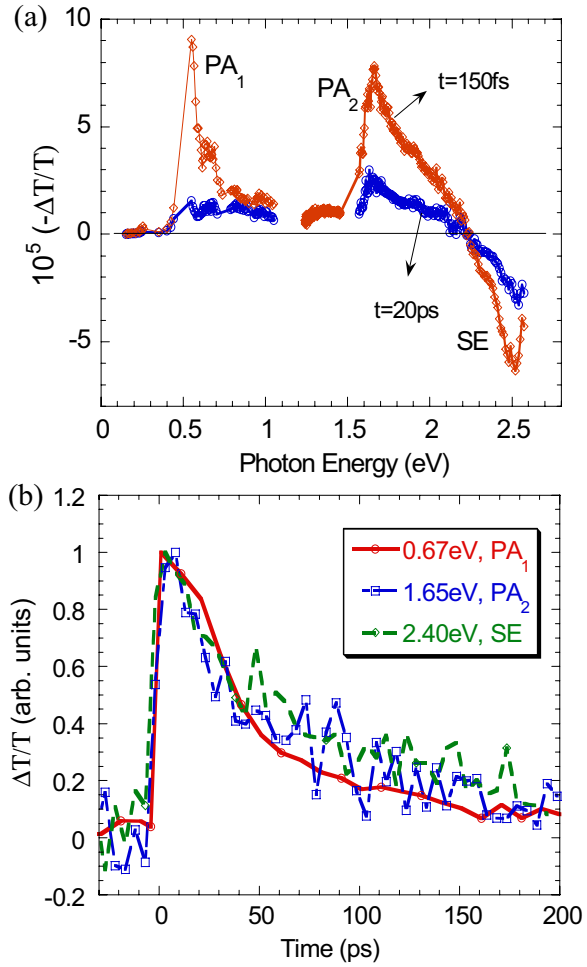

FIG. 6. (Color online) (a) The transient PM spectra of PFO at $t=0$ (red line, diamonds) and $t=20$ ps (blue line, circles). The PA bands PA_1, PA_2, and SE are assigned. (b) The transient decay dynamics of the main bands assigned in (a).

agreement with that of the EA spectrum discussed above. This is not surprising since both NLO spectra are related to the same $\chi^{(3)}$ coefficient, thus reflecting its anisotropy, which is caused by the quasi-1D properties of the polymer chains. The two TPA spectra were fitted using the same SOS, where TAP $\sim$Im $\chi^{(3)}$ $(\omega;\omega, -\omega, \omega)$, with the same parameters as for the fit to the EA spectrum (Table I); no extra parameter is needed. The agreement between the obtained spectrum and the model calculation is excellent. This validates the use of the SOS model and its parameters.

D. Transient photomodulation spectroscopy

We measured the polarized pump and probe PM spectra in a broad spectral range from 0.2 to 2.6 eV using two different laser systems, as discussed in the Experiment section. Figure 6(a) shows the full PM spectrum of a PFO film at two delay times, $t=0$ and $t=20$ ps. The PM spectrum contains two PA bands (PA_1 and PA_2) at 0.55 and 1.65 eV, respectively, and a SE band that peaks at 2.5 eV. We also measured that the parallel PM spectrum $[\Delta T(\text{pa})]$ is $\sim$2.2 times stronger than the perpendicular spectrum $[\Delta T(\text{pe})]$, similar to the parallel-perpendicular ratio in the other two NLO spectra, namely, the EA and TPA in Figs. 3(b) and 5, respectively. It is also seen that PA_1 broadens considerably with time; however, the two PA bands and the SE retain their relative intensity to each other. In particular, the three bands' decay dynamics are shown in Fig. 6(b); the decay dynamics of all three bands are equal, with a lifetime of $\sim$100 ps. This shows that the PM bands belong to the same photogenerated species, in contrast to earlier conclusions.[18] Since SE is related to excitons, we thus attribute this species to photogenerated singlet excitons, namely, $1B_u$. We therefore conclude that the two PA bands are optical transitions from $1B_u$ to the two most strongly coupled A_g excitons in the singlet manifold, namely, mA_g and kA_g, respectively. No hot excitons[18] or polarons[19] are needed to interpret this spectrum. Thus, the three NLO spectroscopies, namely, EA, TPA, and transient PM, are in agreement with each other and show that few dominant states are sufficient to understand the NLO spectra in PFO.

At $t=0$, the PA_1 band is narrower [FWHM=0.2 eV, Fig. 6(a)] than the TPA band (FWHM$\sim$0.4 eV, Fig. 5), although the two transitions are to the same final state: PA_1 is due to transition $1B_u \rightarrow mA_g$, whereas TPA is caused by transition $1A_g \rightarrow mA_g$. However, at a later time [$t=20$ ps, Fig. 6(a)], PA_1 broadens to about 0.4 eV, with width comparable to that of the TPA band. The broad TPA spectrum is caused by the inhomogeneities of $E(1A_g)$ and $E(mA_g)$ in the PFO chains, whereas for PA_1 the inhomogeneities in $E(1B_u)$ and $E(mA_g)$ are involved. However, the TPA is an *equilibrium* process where all PFO chains are excited with equal probability, similar to the absorption process discussed in Sec. III A (Fig. 1), whereas in the transient PM process at $t=0$, not all $1B_u$ excitons in the PFO chains are initially excited with equal probability, since it is a *nonequilibrium* process. Upon photoexcitation, only a narrow subset of the inhomogenously broadened $E(1B_u)$ distribution is actually photoexcited, and this explains the relatively narrow PA_1 band at $t=0$. At a later time, excitons diffuse among the polymer chains and occupy a larger $E(1B_u)$ subset in the distribution; this leads to a broader PA_1 at $t=20$ ps [Fig. 6(a)].

In contrast to PPV derivatives,[5,6,9] the femtosecond transient PM spectrum of PFO does not show any other band that may be related to photogeneration of charge polarons. Our results are in agreement with the lack of long-lived polaron photogeneration in as spun (i.e., glassy α phase) PFO film measured by the cw PM technique.[14] This is in agreement with the large exciton *intrachain* binding energy that we found here for PFO. Also, it clearly indicates that the bulky PFO side groups do not allow strong interchain interaction, which is largely responsible for polaron photogeneration in π-conjugated polymer films.[11] Another possibility for the lack of polaron photogeneration here is the proximity of the laser excitation photon energy ($\sim$3.1 eV) to the absorption onset of PFO ($\sim$3.0 eV).[23] From the excitation dependence of charge photogeneration in PFO using cw PM spectroscopy, it was found[14] that the quantum efficiency of polaron photogeneration dramatically increases at photon energies close to $E(mA_g) \sim 3.7$ eV; up to this photon energy, there is basically very little steady-state photogenerated polarons. We thus expect dramatic changes to occur in the transient PM

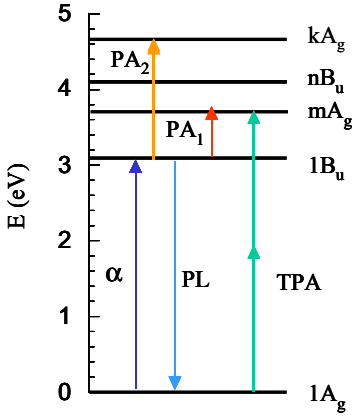

FIG. 7. (Color online) The most important intrachain energy states and allowed optical transitions for PFO. The PA bands are excited state absorptions, α and TPA is linear and NLO absorption, respectively, and PL may be also replaced by SE in the pump-probe experiment.

spectrum of PFO at *higher* excitation photon energies,[23] and/or when the glassy phase changes into a more ordered phase,[20] and when a strong electric field such as in organic light-emitting diodes made of PFO is capable of exciton dissociation even at relatively low excitation photon energy close to $E(1B_u)$.[52]

IV. SUMMARY

We used a variety of linear and nonlinear optical spectroscopies for studying the excited states and photoexcitations of the important polymer PFO having blue PL emission. The NLO spectroscopies included electroabsorption, two-photon absorption, and ultrafast photomodulation, whereas the linear spectroscopies were PL emission and absorption. We found that the excited states of PFO are dominated by four essential states that determine the NLO spectra. These are both odd and even parity excitons: $1B_u$, mA_g, nB_u, and kA_g. Their energies and optical dipole moments were determined by a summation over states model that was used to fit the obtained EA and TPA spectra for $\hbar\omega < 4.5$ eV (Table I) and by inspection of the EA and transient PM spectra at higher energies. These important states are summarized in Fig. 7. Including the $1A_g$, all five states contribute to the EA spectrum, but only the A_g states are seen in the TPA spectrum and in the transitions from $1B_u$ to upper states in the transient PM spectrum.

The PFO polymer cannot be described by the semiconductor band model. The best evidence for this is the comparison between the TPA and linear absorption spectra. The two spectra peak at energies that are ~0.5 eV apart; moreover, the TPA is close to zero at the peak location of the linear absorption. This is impossible to explain by the band model. Another strong indication that PFO is excitonic in nature is the characteristic properties of the primary photoexcitations. These are excitons with two strong PA bands in the mid- and near-IR spectral ranges and a SE band in the visible spectral range, rather than a typical Drude free carrier absorption that characterizes photogenerated carriers in more usual 3D semiconductors such as Si and GaAs. Also, the EA spectrum does not contain any FK oscillation at the continuum band edge, but instead shows derivative-like features of the main excitons, and transfer of oscillator strength to the most strongly coupled A_g states.

From the energy difference between $E(nB_u)$ and $E(1B_u)$ in the excited state spectrum, we estimate the lowest exciton binding energy $E_b \sim 1$ eV. This large "intrachain binding energy" indicates a strongly bound exciton. Such an exciton "steals" most of the oscillator strength from the interband transition.[35] Indeed, there is a huge factor of ~100 between the excitonic transition $1A_g \rightarrow 1B_u$ compared to the interband transition, which we identify here as the $1A_g \rightarrow nB_u$ transition. We also obtained the polarizability of the lowest-lying exciton; it is ~5000 Å^3, which gives an exciton wave function extent in the PFO chains of a few repeated units. The seeming contradiction between the obtained exciton wave function extent and the large intrachain binding energy may be explained by the 1D character of the excitons in PFO.

ACKNOWLEDGMENTS

This work was supported in part by the DOE under Grant No. FG-02 ER46109 and the NSF DMR under Grant No. 05-03172 at the University of Utah. We thank Randy Polson for the help with the measurements and Matt Delong for the help with the sample films. Some of the work was completed at the John Dixon Laser Institute, and we thank the support of University of Utah for this Institute.

*Author to whom correspondence should be addressed; electronic address: val@physics.utah.edu

[1] *Handbook of Conducting Polymers*, 2nd edition, edited by T. A. Skotheim, R. L. Elsenbaumer, and J. R. Reynolds (Dekker, New York, 1998).
[2] S. R. Forrest, Nature (London) **428**, 911 (2004).
[3] G. Malliaras and R. Friend, Phys. Today **58** (5), 53 (2005).
[4] *Primary Photoexcitations in Conjugated Polymers: Molecular Exciton Versus Semiconductor Band Model*, edited by S. Sariciftci (World Scientific, Singapore, 1997), and references therein.
[5] P. B. Miranda, D. Moses, and A. J. Heeger, Phys. Rev. B **64**, 081201(R) (2001).
[6] P. B. Miranda, D. Moses, and A. J. Heeger, Phys. Rev. B **70**, 085212 (2004).
[7] H. Zhao, S. Mazumdar, C. -X. Sheng, M. Tong, and Z. V. Vardeny, Phys. Rev. B **73**, 075403 (2006), and references therein.
[8] M. Yan, L. J. Rothberg, F. Papadimitrakopoulos, M. E. Galvin, and T. M. Miller Phys. Rev. Lett. **72**, 1104 (1994).
[9] E. Hendry, M. Koeberg, J. M. Schins, L. D. A. Siebbeles, and M. Bonn, Phys. Rev. B **70**, 033202 (2004).

[10] T. Virgili, D. Marinotto, C. Manzoni, G. Cerullo, and G. Lanzani, Phys. Rev. Lett. **94**, 117402 (2005).
[11] E. Hendry, M. Koeberg, J. M. Schins, H. K. Nienhuys, V. Sundström, L. D. A. Siebbeles, and M. Bonn, Phys. Rev. B **71**, 125201 (2005).
[12] A. Grice, D. D. C. Bradley, M. T. Bernius, M. Inbasekaran, W. W. Wu, and E. P. Woo, Appl. Phys. Lett. **73**, 629 (1998).
[13] M. Redecker, D. D. C. Bradley, M. Inbasekaran, and E. P. Woo, Adv. Mater. (Weinheim, Ger.) **9**, 798 (1997).
[14] A. J. Cadby, P. A. Lane, H. Mellor, S. J. Martin, M. Grell, C. Giebeler, D. D. C. Bradley, M. Wohlgenannt, C. An, and Z. V. Vardeny, Phys. Rev. B **62**, 15604 (2000).
[15] A. Hayer, A. L. T. Kahn, R. H. Friend, and A. Köhler, Phys. Rev. B **71**, 241302(R) (2005).
[16] M. Redecker, D. D. C. Bradley, M. Inbasekaran, and E. P. Woo, Appl. Phys. Lett. **74**, 1400 (1999).
[17] M. N. Shkunov, R. Österbacka, A. Fujii, K. Yoshino, and Z. V. Vardeny, Appl. Phys. Lett. **74**, 1648 (1999).
[18] S. Xu, V. I. Klimov, B. Kraabel, H. Wang, and D. W. McBranch, Phys. Rev. B **64**, 193201 (2001).
[19] M. A. Stevens, C. Silva, D. M. Russell, and R. H. Friend, Phys. Rev. B **63**, 165213 (2001).
[20] O. J. Korovyanko and Z. V. Vardeny, Chem. Phys. Lett. **356**, 361 (2002).
[21] A. Gambetta, T. Virgili, and G. Lanzani, Appl. Phys. Lett. **86**, 253509 (2005).
[22] X. Zhang, Y. Xia, R. Friend, and C. Silva, Phys. Rev. B **73**, 245201 (2006).
[23] L. Lüer, C. Manzoni, H.-J. Egelhaaf, G. Cerullo, D. Oelkrug, and G. Lanzani, Phys. Rev. B **73**, 035216 (2006).
[24] P. Najechalski, Y. Morel, O. Stephan, and P. L. Baldeck, Chem. Phys. Lett. **343**, 44 (2001).
[25] S. N. Dixit, D. Guo, and S. Mazumdar, Phys. Rev. B **43**, 6781 (1991).
[26] M. Liess, S. Jeglinski, Z. V. Vardeny, M. Ozaki, K. Yoshino, Y. Ding, and T. Barton, Phys. Rev. B **56**, 15712 (1997).
[27] S. V. Frolov, M. Liess, P. A. Lane, W. Gellermann, Z. V. Vardeny, M. Ozaki, and K. Yoshino, Phys. Rev. Lett. **78**, 4285 (1997).
[28] C. X. Sheng, Z. V. Vardeny, A. B. Dalton, and R. H. Baughman, Phys. Rev. B **71**, 125427 (2005).
[29] V. I. Klimov and D. McBranch, Opt. Lett. **23**, 277 (1998).
[30] M. Yan, L. J. Rothberg, E. W. Kwock, and T. M. Miller, Phys. Rev. Lett. **75**, 1992 (1995).
[31] M. Chandross, S. Mazumdar, S. Jeglinski, X. Wei, Z. V. Vardeny, E. W. Kwock, and T. M. Miller, Phys. Rev. B **50**, 14702 (1994).
[32] *Semiconductors and Semimetals*, edited by R. K. Willardson and A. C. Beer. Vol. 9 (Academic, New York, 1972).
[33] L. Sebastian, G. Weiser, and H. Bassler, Chem. Phys. **61**, 125 (1981).
[34] G. Weiser, Phys. Rev. B **45**, 14076 (1992).
[35] D. Guo, S. Mazumdar, S. N. Dixit, F. Kajzar, F. Jarka, Y. Kawabe, and N. Peyghamparian, Phys. Rev. B **48**, 1433 (1993).
[36] L. Sebastian and G. Weiser, Phys. Rev. Lett. **46**, 1156 (1981).
[37] Z. Shuai and J. L. Bredas, Phys. Rev. B **44**, 5962 (1991).
[38] W. Barford, R. J. Bursill, and M. Y. Lavrenitiev, J. Phys.: Condens. Matter **10**, 6429 (1998).
[39] A. Shukla, H. Ghosh, and S. Mazumdar, Phys. Rev. B **67**, 245203 (2003).
[40] B. J. Orr and J. F. Ward, Mol. Phys. **20**, 53 (1971).
[41] M. Chandross, S. Mazumdar, M. Liess, P. A. Lane, Z. V. Vardeny, M. Hamaguchi, and K. Yoshino, Phys. Rev. B **55**, 1486 (1997).
[42] M. J. Rice and Yu. N. Garstein, Phys. Rev. Lett. **73**, 2504 (1994).
[43] A. Chakrabarti and S. Mazumdar, Phys. Rev. B **59**, 4839 (1999).
[44] P. Sony and A. Shukla, Phys. Rev. B **71**, 165204 (2005).
[45] S. V. Frolov, Z. Bao, M. Wohlgenannt, and Z. V. Vardeny, Phys. Rev. B **65**, 205209 (2001).
[46] M. Ozaki, E. Ehrenfreund, R. E. Benner, T. J. Barton, K. Yoshino, and Z. V. Vardeny, Phys. Rev. Lett. **79**, 1762 (1997).
[47] W.-S. Fann, S. Benson, J. M. J. Madey, S. Etemad, G. L. Baker, and F. Kajzar, Phys. Rev. Lett. **62**, 1492 (1989).
[48] B. Lawrence, W. E. Turruellas, M. Cha, M. L. Sundheimer, G. I. Stegeman, J. Meth, S. Etemad, and G. Baker, Phys. Rev. Lett. **73**, 597 (1994).
[49] R. K. Meyer, R. E. Benner, M. Ozaki, M. Liess, Z. V. Vardeny, K. Yoshino, Y. Ding, and T. Barton, Synth. Met. **84**, 549 (1997).
[50] S. Polyakov, F. Yoshino, M. Liu, and G. Stegeman, Phys. Rev. B **69**, 115421 (2004).
[51] C. J. Baker, O. M. Gelsen, and D. D. C. Bradley, Chem. Phys. Lett. **201**, 127 (1993).
[52] T. Virgili, G. Cerullo, C. Gadermaier L. Lüer, G. Lanzani, and D. D. C. Bradley, Phys. Rev. Lett. **90**, 247402 (2003).